JOURNAL OF MATERIALS SCIENCE 35 (2000) 6161–6168

Characterization of dislocations in copper electrodeposits

Y.-S. LEE, D. N. LEE*
School of Materials Science and Engineering, College of Engineering, Seoul National University, Seoul 151-742, South Korea
E-mail: dnlee@snu.ac.kr

Copper electrodeposits with the [111] orientation were obtained from a copper sulfate bath consisting of 280 g/l $CuSO_45H_2O$ and 80 g/l H_2SO_4 at 30°C. The cathode current density was 900 to 1300 A/m^2. Dislocations in the electrodeposits were characterized using transmission electron microscopy. Dislocations in each of the (111) grains could be classified into two groups. One group belonged to high density dislocation bundles radiating from one small area, and another group was located between the bundles. The dislocations in the first group were directed along the ⟨112⟩ directions parallel to the (111) plane and of the edge type. About 42 pct of the dislocations in the second group were also parallel to the (111) plane and of the mixed type. In summary, the majority of dislocations in the (111) grains was of edge type lying on the (111) plane.

1. Introduction

The electrodeposits contain defects such as dislocations, twins, grain boundaries and others. The stored energy due to these defects may provide the driving force for recrystallization of the deposits when annealed. The recrystallization textures may differ from the deposition textures. One of the present author [1] advanced a model for the evolution of the recrystallization texture of deformed metals. In the model, the absolute maximum internal stress direction in the deformed or fabricated metals becomes parallel to the direction of the minimum elastic modulus of recrystallized grains, whereby the release of the strain energy due to dislocations generated during fabrication can be maximized. The strain energy release maximization model could explain the recrystallization textures of deformed metals [1–5] and even copper electrodeposits [6].

It is well known that the electrodeposits have high dislocation densities similar to plastically deformed metals. These dislocations provide a driving force for recrystallization of materials when annealed. The Burgers vector directions of dislocations in an electrodeposit cannot be random and may be determined from its texture. The absolute maximum internal stress direction is the same as the Burgers vector direction in case of an array of parallel edge dislocations [1, 7]. Therefore, the absolute maximum internal stress direction can be determined from the deposition texture. There can be many Burgers vector directions in a crystals, for example, there are six Burgers vector directions, the ⟨110⟩ directions, in fcc metals. However, Lee [8] presumed that the density of dislocations whose Burgers vectors are directed away from the thickness direction would be higher than that of dislocations whose Burgers vector are approximately parallel to the thickness direction, because dislocations whose Burgers vector is close to the thickness direction would glide out from the deposit by the image force during its growth. Therefore, the Burgers vector directions at right angles or near right angles to the thickness direction of the original deposit would determine the absolute maximum internal stress direction of deposits.

This concept could explain the recrystallization textures of copper [6, 8], chromium [9] and silver [10] electrodeposits. However, the presumption on dislocations has never been experimentally proved. The objective of this study is to investigate characteristics of dislocations in copper electrodeposits.

2. Experimental

Copper electrodeposition was carried out in a copper sulfate bath consisting of 280 g/l $CuSO_45H_2O$ and 80 g/l H_2SO_4 at 30°C with four different cathode current densities of 700, 900, 1100, and 1300 A/m^2. Stainless steel and lead sheets were used as cathode and anode, respectively. The thickness of copper electrodeposits was ranged from 40 to 65 μm.

Specimens for transmission electron microscopy (TEM) were cut into 3 mm diameter discs from the deposit and thinned in a solution of 33 Vol.% nitric acid and 67 Vol.% methanol at 15°C. Transmission electron microcopy was carried out in Philips CM20 instruments operating at 200 kV. In addition to the conventional bright field method, a weak beam dark field (WBDF) technique was used to obtain a high resolution of dislocation images.

* Author to whom all correspondence should be addressed.

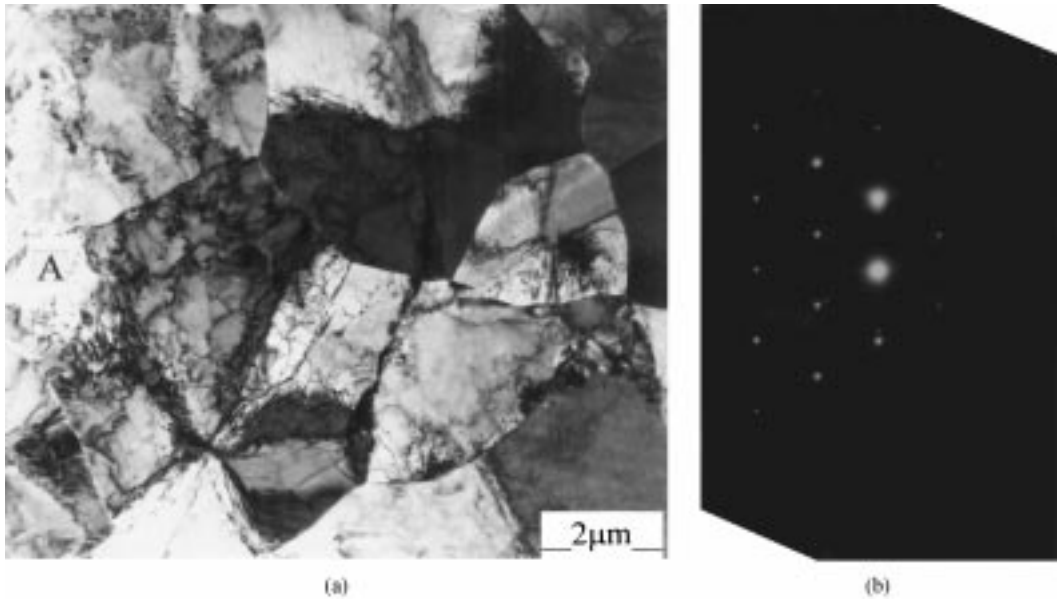

Figure 1 (a) TEM micrograph showing (111) grains in copper electrodeposit obtained at 1300 A/m^2. Electron beam is parallel to ⟨111⟩. (b) SAD pattern from Grain A in (a).

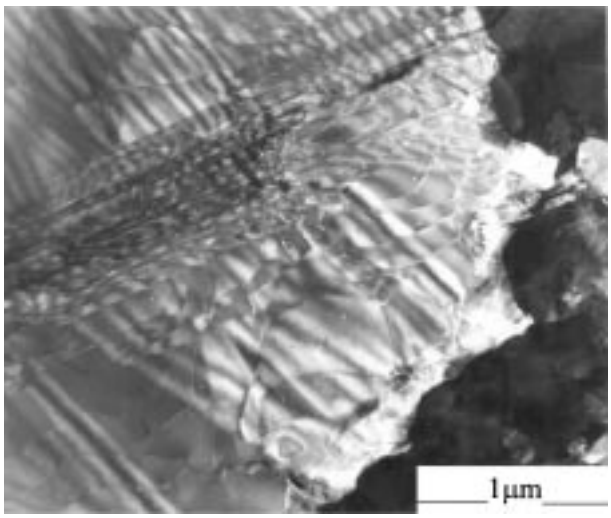

Figure 2 Weak Beam Dark Field TEM micrograph showing dislocation bundle in (111) grain. Electron beam is approximately parallel to ⟨110⟩.

In order to define the preferred orientation of the growth direction of copper deposits, X-ray diffraction (XRD) was applied at 50 kV and 100 mA using Cu target. The orientation of the deposits was expressed by the texture fraction, which is defined by

$$\mathrm{TF} = \frac{I(\mathrm{hkl})/\mathrm{Io(hkl)}}{\sum[I(\mathrm{hkl})/\mathrm{Io(hkl)}]}$$

where I(hkl) is the integrated intensity of (hkl) reflection measured for experimental specimens and Io(hkl) is that for a standard powder sample.

Two techniques were applied to carry out quantitative analysis of dislocations. The Burgers vectors of dislocations were determined by the invisibility criterion, in which dislocation images are invisible when $\boldsymbol{g}\cdot\boldsymbol{b} = 0$ with $\boldsymbol{g}$ and $\boldsymbol{b}$ being a reflection and the Burgers vector, respectively. To experimentally determine types of dislocations, the dislocation line direction $\boldsymbol{u}$ as well as the Burgers vector should be identified. The direction $\boldsymbol{u}$ can be determined by the trace analysis method described in the following: (i) Take photographs of a dislocation with different beam directions. (ii) Overlap the diffraction patterns on each micrograph and mark traces of a suitable reflecting plane. (iii) Measure the angle

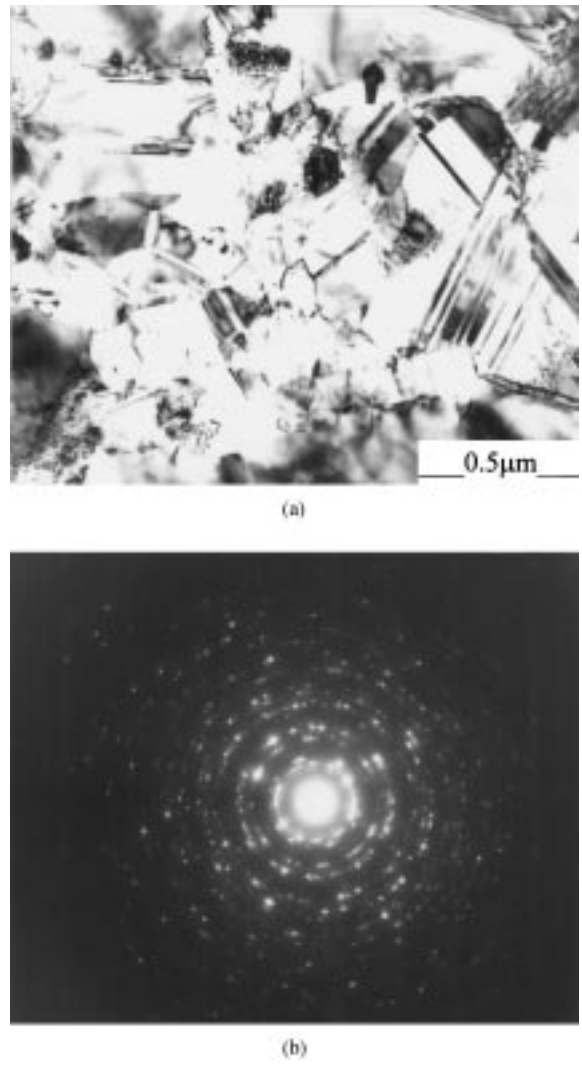

Figure 3 (a) TEM micrograph showing other grains in copper electrodeposit obtained at 1300 A/m^2. (b) SAED pattern from area with fine grains.

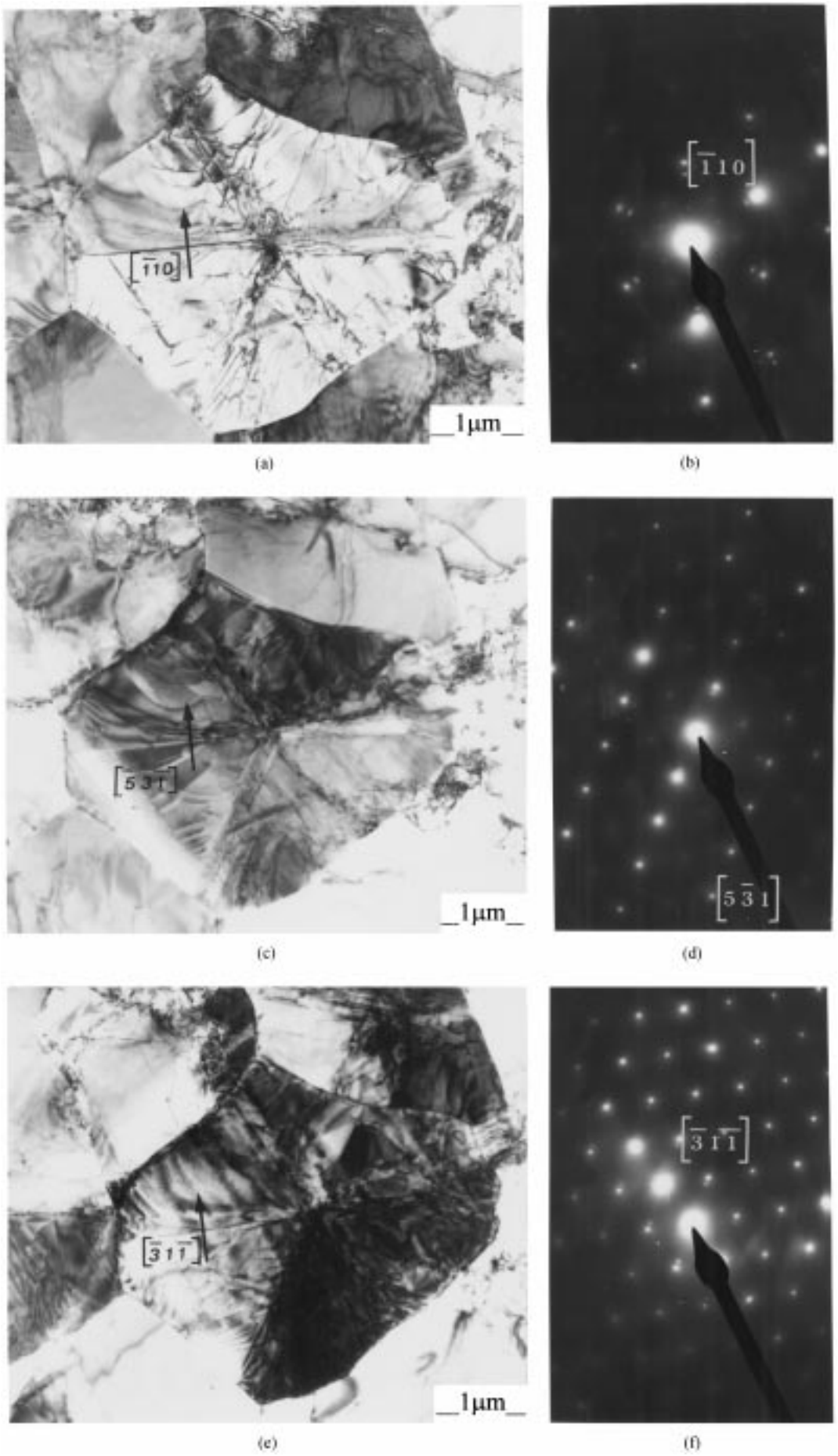

Figure 4 TEM micrographs showing (111) grain recorded parallel to (a) [111], (c) [121], and (e) [011]. Corresponding SAED patterns are shown in (b), (d) and (f), respectively.

between the plane chosen and the normal to the projected line direction of the dislocation for all cases. (iv) Plot these normals on the stereographic projection using the exact beam direction for the micrographs and the angles. (v) Construct a great circle including the normals. The pole of this great circle is the line direction of the dislocation.

3. Results

3.1. Macrotexture

The data in Table I indicate that the texture fraction of (111) plane increased with increasing current density from 700 to 1300 A/m^2, whereas the texture fraction of (110) showed the opposite trend. The orientations of grains in the sample obtained at 1300 A/m^2 were predominantly [111], with minor fraction of [100] and [110]. Lee *et al.* (recent review [11]) suggested that the development of (111) texture at high current densities was due to a decrease in the copper ion concentration adjacent to the cathode, because the depletion rate of copper ion due to reduction at cathode was higher than the diffusion rate of copper ion to the cathode. In the present work, the study has been focussed on the specimen obtained at 1300 A/m^2, because of its high texture fraction of (111).

TABLE I Texture fractions in copper electrodeposits

Current Density (A/m^2)	TF		
	(111)	(100)	(110)
900	0.679	0.125	0.196
1100	0.785	0.077	0.138
1300	0.877	0.032	0.091

3.2. Microstructure

Typical microstructures of the deposits obtained at 1300 A/m^2 consisted of two distinct areas as shown in Figs 1–3. The microstructure in Fig. 1 contains relatively coarse grains, which have radial type fragments diverging three directions separated by about 60°. It is interesting to note that the (111) grains are divided into 4 to 6 sectors. The electron microdiffraction pattern in Fig. 1b taken from the central part of the grain A in (a) is Cu [111] zone axis. The image of the same specimen with higher magnification, Fig. 2, shows that the boundaries spreading in the radial direction are the 'bundles' of a high density of straight dislocations. An analysis of the image and the corresponding diffraction pattern showed that the projected dislocation bundles were parallel to ⟨112⟩ directions. Different contrast from individual fragment seperated by the dislocation bundles indicates that the fragments in the same grain have misorientation with each other. The observation of the Kikuchi patterns from each fragment revealed that the misorientation angle between the fragments was about 5°, which indicates that the dislocation bundles may be made of low angle boundaries. In contrast, areas located between the dislocation bundles have much less dislocation density.

In addition to coarse (111) grains, fine grain clusters in fractions were also observed as shown in Fig. 3. The

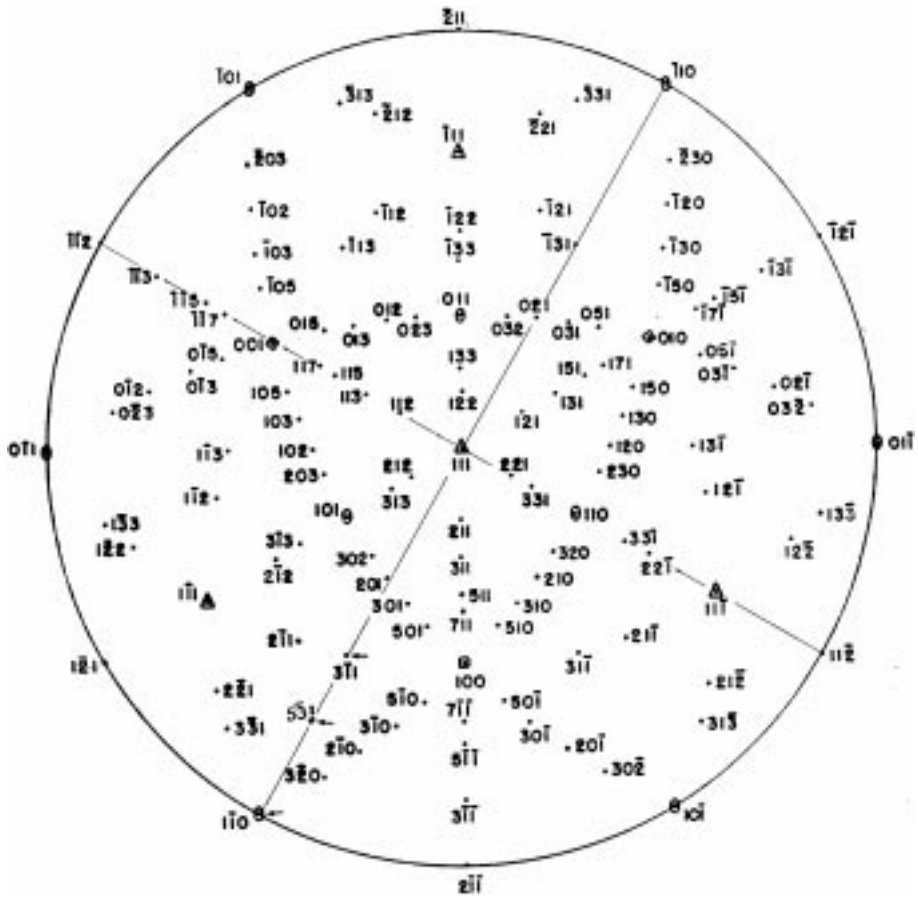

Figure 5 Stereographic projection showing pole of the great circle including three normals in Fig. 4.

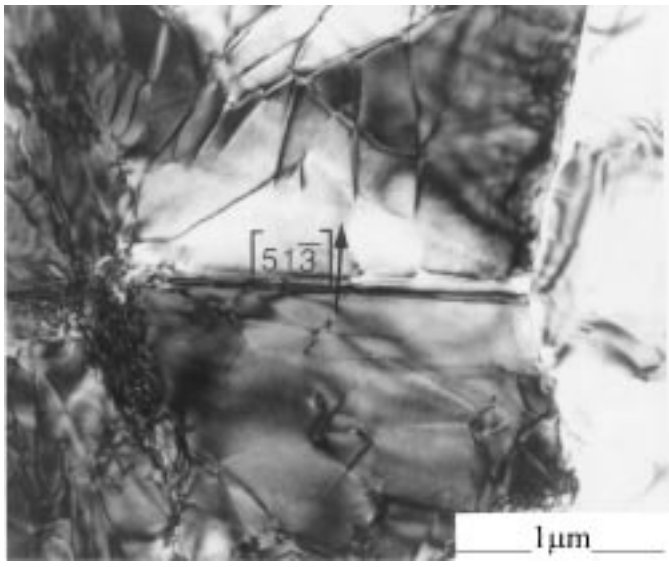

(a)

(b)

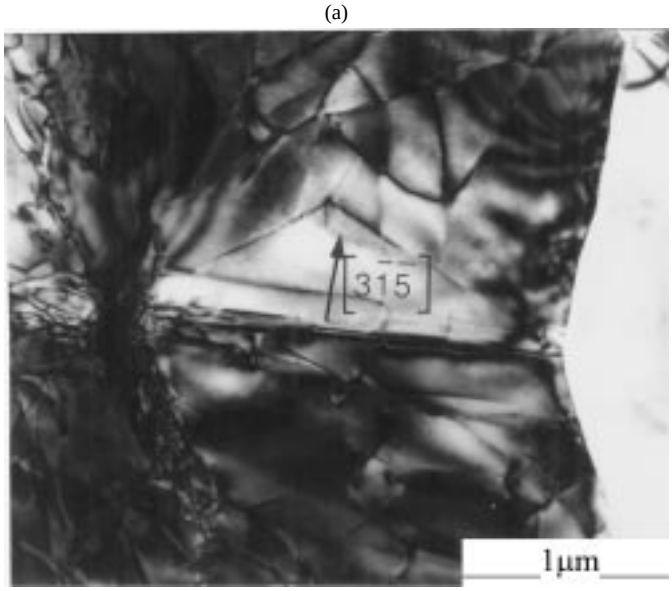

(c)

(d)

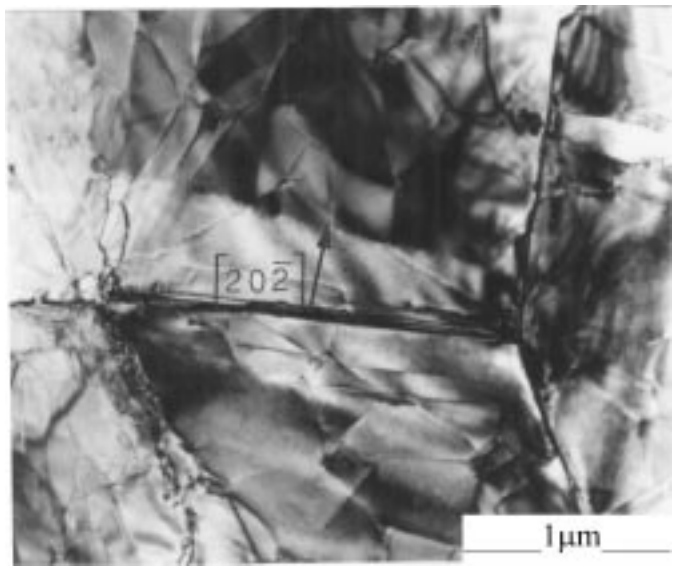

(e)

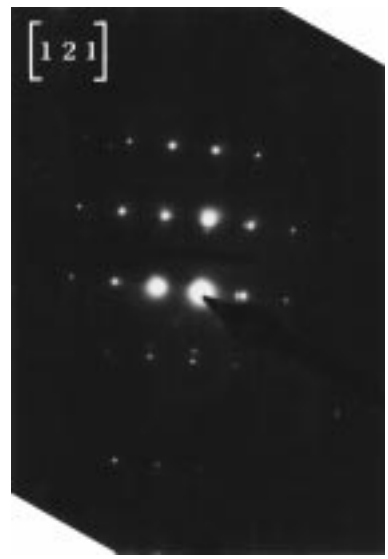

(f)

Figure 6 TEM micrographs showing (111) grain recorded parallel to (a) [112], (c) [211], and (e) [121]. Corresponding SAED patterns are shown in (b), (d) and (f), respectively.

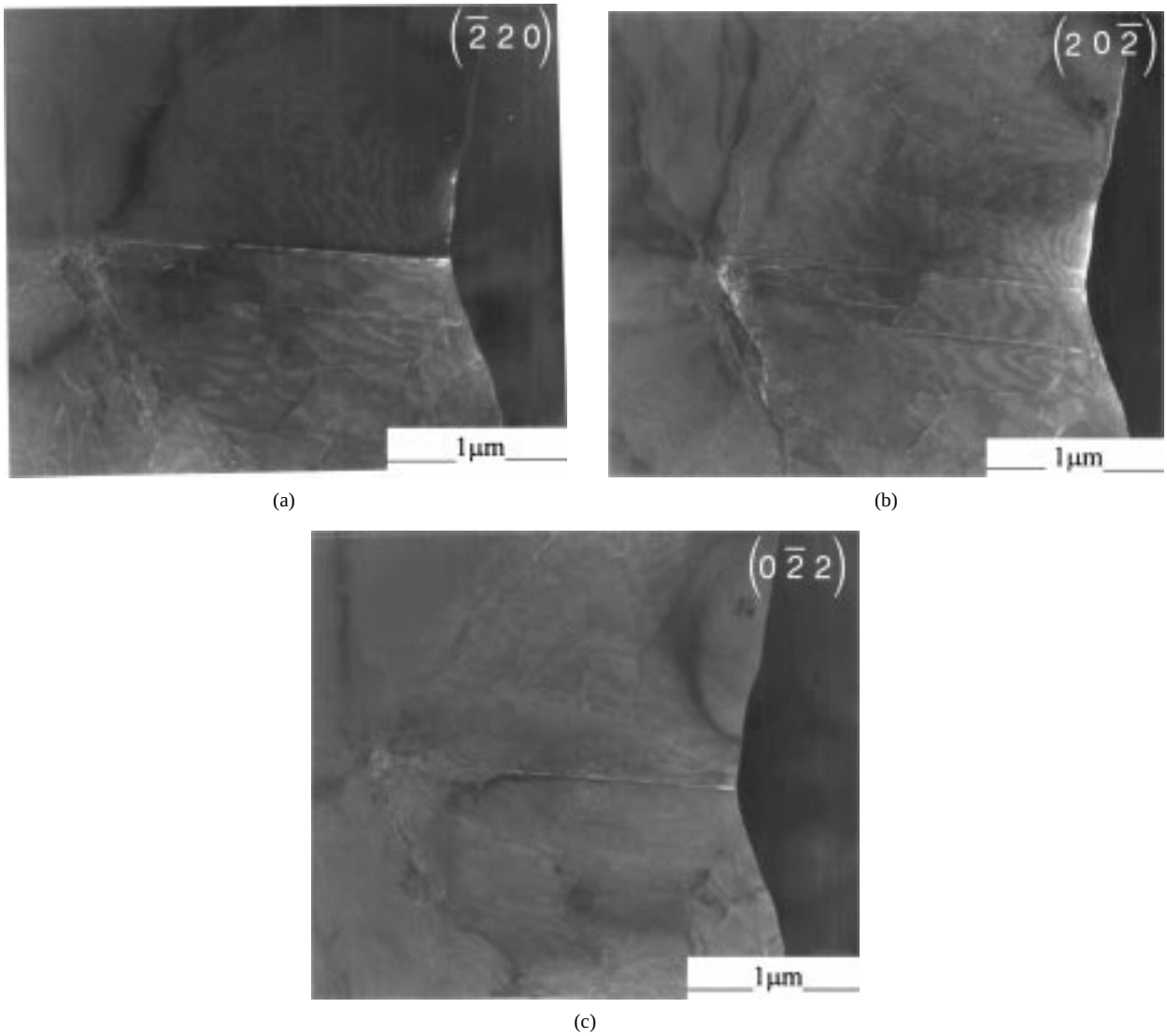

Figure 7 Weak Beam Dark Field TEM micrographs showing straight dislocation bundle in Fig. 6 recorded with different $\boldsymbol{g}$ vectors. (a) $(\bar{2}20)$, (b) $(20\bar{2})$ and (c) $(0\bar{2}2)$.

Debye rings in selected area diffraction pattern (SADP) recorded from the cluster is an evidence for the polycrystalline structure. The investigation into electron microdiffraction patterns from individual grains confirmed that the clusters have grains with different deposition growth directions, such as [110], [100] and [112].

3.3. Quantitative analysis of dislocations

A quantitative analysis of dislocations was carried out at two distinct regions, dislocation bundles and regions between the bundles. Since dislocation images recorded in TEM are two-dimensional projected ones, the dislocation line directions $\boldsymbol{u}$ should be determined to identify their types. Straightness of dislocations in the bundles allows us to determine the type of dislocations using the trace analysis method which is described in the Experimental. Fig. 4a, c, and e show the images of an individual dislocation bundle taken at zone axes parallel to [111], [121], and [011], respectively. The examination of images and corresponding diffraction patterns in Fig. 4b, d, and f revealed that the normal directions of the projected image (arrowed) of the dislocation bundle at the different zone axes are parallel to the reflections $[\bar{1}10]$, $[\bar{5}3\bar{1}]$ and $[\bar{3}1\bar{1}]$, respectively. The great circle including the reflections was constructed on the stereographic projection as shown in Fig. 5. Since the normal of the great circle is the line vector of the dislocations in the bundle, it is concluded that the dislocation line vector $\boldsymbol{u}$ is parallel to the $[11\bar{2}]$ direction. Using the same method, line vectors of other two dislocation bundles were identified as $[\bar{2}11]$ and $[\bar{1}21]$. Another example is shown in Fig. 6, in which a dislocation bundle of interest was taken at zone axes parallel to [112], [211] and [121]. The examination of images and corresponding diffraction patterns in Fig. 6b, d, and f revealed that the reflections, $[51\bar{3}]$, $[3\bar{1}5]$, and $[20\bar{2}]$, were parallel to the normal directions of the projected image (arrow) of the dislocation bundle at different zone axes. A great circle including the normal directions was constructed on the stereographic projection in Fig. 5. Since the normal of the great circle is the line vector of dislocations in the bundle, it is concluded that the dislocation line vector $\boldsymbol{u}$ is parallel to the $[1\bar{2}1]$ direction. With the same method, line vectors of other two dislocation bundles were identified as $[\bar{2}11]$ and $[\bar{1}12]$. The examination of other (111) grains also indicated that dislocation bundles are parallel to $\langle 112 \rangle$ direction. It is therefore

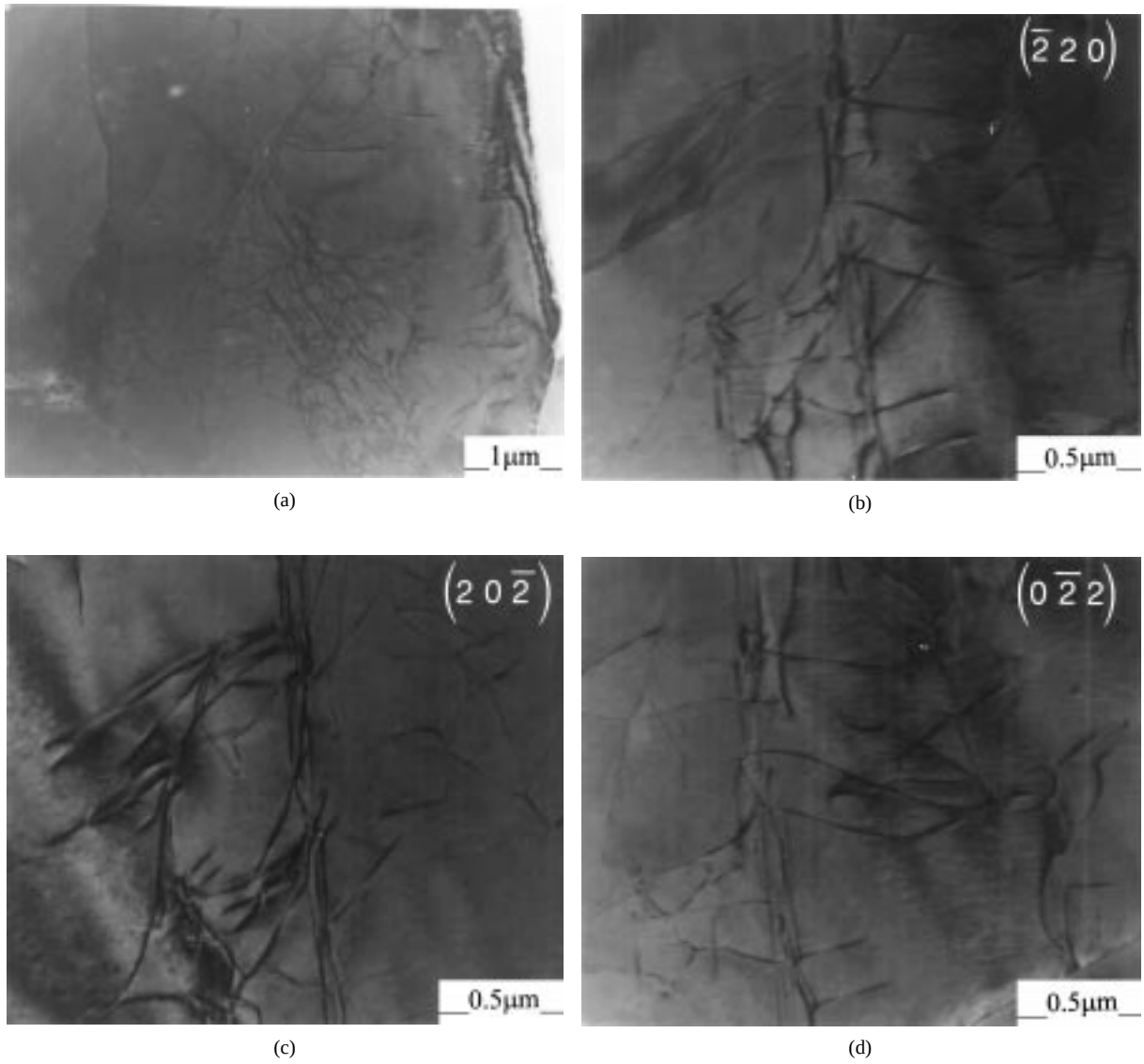

Figure 8 TEM micrographs showing dislocation bundle in copper electrodeposit obtained at 900 A/m^2, recorded with different $\boldsymbol{g}$ vectors. (a) $(\bar{2}20)$, (b) $(20\bar{2})$ and (c) $(0\bar{2}2)$.

concluded that dislocations consisting of the bundles are on the (111) plane.

The Burgers vector $\boldsymbol{b}$ of dislocations in the bundles was very difficult to identify because their close-packing produced a poor image contrast. A bundle with a low dislocation density was selected to determine $\boldsymbol{b}$ of dislocations. WBDF electron micrographs in Fig. 7 were recorded from an individual (111) grain with three different two-beam conditions, in which reflections were parallel to (a) $(\bar{2}20)$, (b) $(20\bar{2})$, and (c) $(0\bar{2}2)$, respectively. It is noted that the straight dislocations arrowed are visible with all the three $\boldsymbol{g}$ above. In the face centred cubic system, when dislocations are of the type $\boldsymbol{b} = 1/2[\bar{1}10]$, $1/2[10\bar{1}]$ or $1/2[0\bar{1}1]$ which lie down on the (111) plane, dislocation images are visible at the $(\bar{2}20)$, (202) and (022) reflections. This result confirms that the direction of the dislocations in the bundles is perpendicular to the normal of the (111) planes.

In summary, the directions of dislocations in the bundles are parallel to $[2\bar{1}1]$, $[11\bar{2}]$ and $[\bar{1}21]$, and the Burgers vectors are $1/2[\bar{1}10]$, $1/2[10\bar{1}]$ and $1/2[0\bar{1}1]$. Therefore, $\boldsymbol{b} = 1/2[\bar{1}10]$, $1/2[10\bar{1}]$ and $1/2[0\bar{1}1]$ are perpendicular to $[11\bar{2}]$, $[\bar{1}21]$ and $[2\bar{1}1]$, respectively, that is, the Burgers vectors are normal to the dislocation lines, indicating that the bundles consist of edge dislocations. The above results were also observed in the sample deposited at 900 A/m^2. The typical microstructure of the sample obtained at 900 A/m^2 was identical to that at 1300 A/m^2, as shown in Fig. 8a. The grain in Fig. 8a also contained the dislocation bundles expanding from the central part with radial directions separated by 120°, whereas the density of dislocations was remarkably low compared to that of the sample deposited at 1300 A/m^2. It has been determined that the line direction of the dislocation bundles in the 900 A/m^2 sample was approximately parallel to $[2\bar{1}1]$, $[11\bar{2}]$ or $[\bar{1}21]$, as observed in the 1300 A/m^2 sample.

In a case of the region with the lower density of dislocations, it was difficult to identify their type because they mainly existed as a mixed type. The examination of the Burgers vectors of approximately 300 dislocations existing between the dislocation bundles using the invisibility criterion showed that approximately 42% of the dislocations had $\boldsymbol{b} = 1/2[\bar{1}10]$, $1/2[10\bar{1}]$ or $1/2[0\bar{1}1]$ which lie on the (111) plane.

In addition, the possibility that the dislocations bundles may consist of partial dislocations should be considered. For the (111) foil, partial dislocations are on the $(\bar{1}11)$ plane, with a Burgers vector of $1/6[\bar{2}11]$, $1/6[\bar{1}21]$, or $1/6[11\bar{2}]$ for the Shockely partials, and 1/3[111] for the Frank partials. The kinematical and dynamical theories of electron diffraction have established that partial dislocations become invisible when $\boldsymbol{g}\cdot\boldsymbol{b}_{\mathrm{p}} = 0$, where $\boldsymbol{b}_{\mathrm{p}}$ is the Burgers vector of the partial dislocations, but there is an added complication that they exhibit weak contrast when $\boldsymbol{g}\cdot\boldsymbol{b}_{\mathrm{p}} = 1/3$. It should be noted that dislocation image is always visible at three different reflections, $(\bar{2}20)$, $(20\bar{2})$, and (022). This result denies the possibility that dislocation bundles consist of partial dislocations. If dislocations in bundles are the Shockely partials, the invisibility should exist for one of these reflections, because partial dislocations in fcc materials are visible for $\boldsymbol{g}\cdot\boldsymbol{b}_{\mathrm{p}} = 1/3$ and 2/3, at $\boldsymbol{s} = 0$ ($\boldsymbol{s}$: deviation parameter). For the Frank, it is invisible for all reflections.

4. Conclusion

A study on transmission electron microscopy of dislocations in copper electrodeposits with the [111] orientation lead to the following conclusion. The majority of dislocations are of edge type with their Burgers vector lying on the (111) plane.

Acknowledgement

This study has been supported by Korea Science and Engineering Foundation.

References

1. D. N. LEE, *Scripta Metall. Mater.* **32** (1995) 1689.
2. *Idem., Texture. Microstruct.* **26-27** (1996) 361.
3. Y. B. PARK, D. N. LEE and G. GOTTSTEIN, *Mater. Sci. Tech.* **13** (1997) 289.
4. S. H. HONG, H.-T. JEONG, C.-H. CHOI and D. N. LEE, *Mater. Sci. Eng.* **A229** (1997) 174.
5. C.-H. CHOI and D. N. LEE, *Metall. Mater. Trans.* **28A** (1997) 2217.
6. D. N. LEE, S.-Y. KANG and J.-S. YANG, *Plating and Surf. Finish.* **82**(March) (1995) 76.
7. A. P. SUTTON and R. W. BALLUFFI, "Interfaces in Crystalline Materials" (Clarendon Press, Oxford, 1996) p. 115.
8. D. N. LEE, *Metals and Mater.* **2** (1996) 121.
9. J.-H. CHOI, S.-Y. KANG and D. N. LEE, *J. Mater. Sci.*, in press.
10. H. S. NAM and D. N. LEE, *J. Electrochem. Soc.* **146** (1999) 3300.
11. D. N. LEE, *MRS Symp. Proc.* **427** (1996) 168.

Received 16 June 1999
and accepted 24 May 2000